Oecologia (1999) 119:300–310

David Ackerly

Self-shading, carbon gain and leaf dynamics: a test of alternative optimality models

Received: 13 October 1998 / Accepted: 27 January 1999

Abstract A simple model of shoot-level carbon gain is presented addressing the optimal number and life span of leaves in relation to alternative optimality criteria: (1) maximizing carbon export from the shoot, or (2) maximizing the rate of leaf production at the shoot tip. Additionally, the processes that cause declining assimilation with leaf age are considered in relation to (1) leaf position on the shoot (e.g., self-shading) versus (2) leaf age per se. Using these alternative scenarios, only a model based on position-dependent assimilation and maximization of leaf production rates resulted in quantitative predictions for all aspects of leaf dynamics on the shoot (i.e., leaf number, life span, and birth rate), while other approaches predicted that one or more parameters would be infinite. This formulation of the model also predicted that leaves should be maintained on the shoot until the diurnal carbon balance declines to zero, in contrast with other scenarios which predict that leaves should be shed while maintaining a positive carbon balance. Predictions of the model were supported by the results of a field study of carbon gain and leaf dynamics in saplings of three species of tropical pioneer trees (*Carica papaya*, *Cecropia obtusifolia*, and *Hampea nutricia*) which differ in the number of leaves per shoot. The results illustrate that in these fast-growing plants, leaf production and height growth may be more appropriate measures of performance than net carbon export from the shoot, and suggest that leaf senescence is primarily a function of the position of a leaf within the canopy, rather than its chronological age.

D. Ackerly (✉)[1]
Department of Organismic and Evolutionary Biology,
Harvard University,
Cambridge, MA 02138, USA

Present address:
[1]Department of Biological Sciences,
Stanford University,
Stanford, CA 94305, USA,
e-mail: dackerly@stanford.edu,
Tel.: +1-650-7230176, Fax: +1-650-7236132

Key words Canopy structure · Carbon assimilation · Leaf life span · Self-shading · Tropical tree

Introduction

Many studies have addressed the factors influencing leaf life span (reviews in Chabot and Hicks 1982; Kikuzawa 1995) and its associations with other aspects of leaf physiology and plant growth (Reich et al. 1992, 1997; Ackerly 1996). Cost-benefit studies of leaf life span have generally treated the leaf as an organ of carbon gain, and have examined the balance of carbon assimilation versus costs of construction and maintenance in different environments (Chabot and Hicks 1982; Williams et al. 1989; Kikuzawa 1991; Sobrado 1991; Kikuzawa and Kudo 1995). Implicit in such studies is the assumption that maximum carbon gain by the individual leaf will also contribute to optimal whole-plant performance. However, leaves also play an important role in plant development which is not addressed by these models. The growth of plant stems, including height growth, depends on the addition and elongation of internodes, and each internode is produced in association with a new leaf. Leaf and internode production depend on carbon availability, but the physiological processes that result in maximum net carbon gain per leaf may not be the same as those that maximize rates of leaf production and height growth. The goal of this paper is to consider the optimal structure and dynamics of individuals shoots with respect to these alternative optimality criteria, and the implications for the life span of leaves.

Cost-benefit models of leaf life span have correctly predicted many trends observed in natural situations, based on assimilation rates and construction costs (e.g., Williams et al. 1989). Kikuzawa (1991) incorporated a senescence parameter as well, describing the decline in net assimilation with leaf age. One prediction of the resulting model is that optimal leaf life span would be infinite if carbon gain did not decline with age, as there would be no reason to drop an old leaf and incur the

construction costs of a new leaf. While it is true that carbon gain declines as leaves age, the mechanisms underlying these patterns may not be based on leaf age per se. At the shoot and whole-plant level, one of the consequences of height growth in canopies is self-shading among leaves, as new leaves are produced in upper-canopy positions and older leaves occupy successively lower and less illuminated positions (Field 1983; Ackerly and Bazzaz 1995a). Self-shading, and the consequent reduction in light levels during the lifetime of a leaf, contributes to declining carbon gain through at least two mechanisms. First, lower light levels directly reduce photosynthetic rates due to energy limitation. Secondly, older leaves exhibit reductions in nitrogen concentration and photosynthetic capacity (Field 1983). Interspecific comparisons across habitats and growth forms illustrate that species with steeper light gradients through the canopy also exhibit a more marked decline in photosynthetic capacity (e.g., Mooney et al. 1981; Witkowski et al. 1992). Similarly, experimental manipulation of light gradients through the canopy alters gradients of nitrogen and assimilation rates (Hirose et al. 1988; Hikosaka et al. 1994) as well as the number (and life span) of leaves maintained on the plant (Ackerly and Bazzaz 1995a). Molecular genetic studies also suggest that declining assimilation rates, as would be caused by shading, precede the expression of senescence-associated genes (Hensel et al. 1993). These observations suggest that the processes responsible for declining carbon gain are primarily related to declining light levels on the leaf, and are therefore dependent on canopy geometry and leaf position rather than leaf age. For the purposes of this study, however, it is sufficient to note that position-dependent and time-dependent processes may be distinguished conceptually, even though both may be at work in the lifetime of an individual leaf.

In this paper, I present a cost-benefit model of leaf dynamics and carbon gain for plants in an aseasonal environment with continuous leaf production. The unit of analysis in this model is the leaf cluster, i.e., the leaves on the tip of an individual branch (cf. Fisher 1986). In tropical plants with continuous aseasonal leaf production, including pioneer trees, palms, tree ferns and cycads, leaf birth and death on each shoot are relatively constant throughout the year (see Ackerly 1996). The balance between the production of new leaves and the loss of old ones results in the maintenance of relatively constant leaf numbers in each cluster, as observed on individual shoots monitored over time and in allometric studies of canopy development (Alvarez-Buylla and Martínez-Ramos 1992; Ackerly 1996). Increases in whole-plant leaf area during growth are primarily due to branching, which increases the number of leaf clusters, and secondarily (especially in young plants) due to increases in individual leaf size. The result of this constant turnover of leaves within the leaf cluster is a simple quantitative relationship between leaf life span (L), number (N) and birth rate (r):

$$L = \frac{N}{r} \tag{1}$$

This is apparent if one considers that the age of the lowest leaf in the leaf cluster (and hence leaf life span) is equal to the product of the position of this leaf relative to the apex (= leaf number) and the time interval between production of successive leaves (= the inverse of leaf birth rate) (Ackerly 1996). By focusing on the leaf cluster, and utilizing this relationship, alternative models were explored based on two optimality criteria (maximization of carbon export from the leaf cluster vs maximization of leaf production rates) and either age-dependent or position-dependent declines in assimilation rates. A preliminary test of the model predictions was then conducted in a field study, based on measurements of leaf dynamics and carbon assimilation in saplings of tropical pioneer trees.

The model

The leaf cluster is comprised of a group of leaves and their associated support structures. Total diurnal assimilation of the cluster, D_g, is allocated among two pools: (1) production of new leaves, including the construction and maintenance costs of leaves, petioles, and internode tissue (D_c) and (2) carbon available for export from the leaf cluster to the subtending branch, the rest of the plant (including belowground), or to reproductive structures (D_s). Assimilation of carbon is quantified in terms of grams of glucose, with a construction cost term (discussed below) to convert from glucose to structural biomass. Total daily assimilation is:

$$D_g = Nma_m \tag{2}$$

where m is individual leaf mass, and a_m is the mean daily assimilation rate of all leaves. Diurnal investment of assimilate in new leaves is:

$$D_c = FNma_m \tag{3}$$

where F is the proportion of total assimilate allocated to new leaf production (symbols and associated units used in the model are summarized in Table 1).

The leaf birth rate at the apex will reflect the carbohydrate allocated to leaf production, divided by the cost of each leaf ($r = D_c/mc$, where c is construction cost, including the structural and respiratory costs of leaf, petiole, and internode per unit of leaf mass). By rearrangement, and substitution of Eq. 1 for r, an alternate definition of D_c is obtained:

$$D_c = (Nmc)/L \tag{4}$$

The net carbon gain of a shoot that is available for export, D_s, is total assimilation (D_g, Eq. 2) minus the cost of leaf production (D_c, Eq. 4),

$$D_s = Nm\left(a_m - \frac{c}{L}\right) \tag{5}$$

Finally, by substituting Eq. 3 into the expression above ($r = D_c/mc$), the rate of leaf birth may be expressed in

Table 1 Summary of parameters used in model equations and appropriate units for each (*glu* glucose, *lf* leaf biomass)

a_0	Initial net assimilation rate of a fully mature leaf	g glu g lf^{-1} day^{-1}
a_m	Mean net assimilation rate of leaves on a shoot	g glu g lf^{-1} day^{-1}
a_x	Net assimilation of leaf at time of abscission	g glu g lf^{-1} day^{-1}
b	Leaf age at which net assimilation reaches zero	days
c	Leaf construction cost	g glu g lf^{-1}
D_c	Daily cost of production of new leaves by shoot	g glu day^{-1}
D_g	Daily gross assimilation by shoot	g glu day^{-1}
D_s	Daily carbon export from shoot	g glu day^{-1}
F	Proportional allocation of assimilate to new leaf production	g glu g glu^{-1}
i	Position of leaf relative to shoot apex	
L	Leaf life span	days
m	Individual leaf mass	g lf
N	Number of leaves on shoot	
p	Leaf position at which net assimilation reaches zero	
r	Leaf birth rate	day^{-1}

terms of assimilation and construction cost (leaf size cancels out of this equation):

$$r = (Na_m F)/c \tag{6}$$

Maximization of Eq. 5 and Eq. 6 defines the two optimality criteria in this study, for 'export' (X) and 'extension' (R) maximizing shoots, respectively. For empirical purposes, the total construction cost is calculated as the sum of leaf biomass, plus support biomass for the duration of a leaf life span (measured as petiole and internode biomass of the lowest leaf on the shoot), each scaled by the respiratory cost of tissue construction; the total cost is then divided by leaf mass to obtain construction and support cost per gram of leaf (c) (Williams et al. 1989; Griffin 1994; costs of subtending branches and roots are considered part of D_s, the export of carbon from the shoot; cf. Kikuzawa and Ackerly, in press).

Mean assimilation rates (a_m) depend on the distribution of rates among leaves on the shoot, which may be a function of leaf age or leaf position. In this model, the decline in assimilation rates is assumed to be linear for simplicity, either as a function of leaf age alone, or of leaf position alone (see Discussion). Following Kikuzawa (1991), the assimilation function is defined by a_0, net assimilation rates of a newly produced leaf, and by the x-intercept which represents either the time (b) or the position (p) at which net assimilation reaches zero. The pattern of shading and consequent decline in assimilation with leaf position will depend on various aspects of canopy geometry, including leaf size, shape and orientation, petiole length and orientation, phyllotaxy, internode length and shoot orientation (Niklas 1988; Takenaka 1994; Pearcy and Yang 1996). In this paper, the effects of these factors are collapsed into the single parameter p and they are not considered explicitly. Mean assimilation rates are the average of the initial and final rates, where L and N define the age and position of the last leaf, respectively, which simplify to the following (see Ackerly 1993):

$$\text{i) age-dependent (A): } a_m = a_0 - \frac{a_0 L}{2b} \tag{7a}$$

$$\text{ii) Position-dependent (P): } a_m = a_0 - \frac{a_0 N}{2p} \tag{7b}$$

By directly substituting these two equations for a_m into each of the optimality criteria defined above (Eqs. 5 and 6), four different equations are obtained (Table 2; Eq. 8) which can then be differentiated with respect to N or L. Predictions of optimal leaf number (N^*) and life span (L^*) for two of the four cases are presented here: the export-maximizing, age-dependent model (XA, Eq. 8a) and the extension-maximizing, position-dependent model (RP, Eq. 8d). From a biological perspective, short shoots may provide a possible example of an export-maximizing (XA) shoot, in which a few leaves are produced but there is not significant extension growth, and this model is mathematically equivalent to that of Kikuzawa (1991) though derived from a slightly different perspective. The RP model examines the consequences of the alternative optimality and leaf-aging criteria introduced in this paper; as argued above, extension-maximizing shoots may be characteristic of the leaders and primary branches of fast-growing trees such as tropical pioneers. The other two scenarios in Table 2 provide somewhat intermediate solutions compared to the two considered here, and are not discussed further (see details in Ackerly 1993). From the solutions

Table 2 Equations that are maximized with respect to leaf life span (L) or number (N) under four different scenarios in this model, based on two different optimality criteria and two patterns of declining assimilation. Numbers in parentheses are equation numbers referred to in the text. See parameter definitions in Table 1. Solutions to Eq. 8a with respect to L and Eq. 8d with respect to N are presented in the text

Assimilation pattern	Optimality criteria Carbon export (X)		Shoot extension (R)	
Age dependent (A)	$D_s = Nm\left(a_0 - \frac{a_0 L}{2b} - \frac{c}{L}\right)$	(8a)	$r = \frac{NFa_0}{c}\left(1 - \frac{L}{2b}\right)$	(8c)
Position dependent (B)	$D_s = Nm\left(a_0 - \frac{a_0 N}{2p} - \frac{c}{L}\right)$	(8b)	$r = \frac{NFa_0}{c}\left(1 - \frac{N}{2p}\right)$	(8d)

in each case, the predicted value of daily leaf assimilation at the time of leaf death (a_x*) can also be calculated, and empirical estimates of this parameter provide one critical test of the alternative models.

Model predictions

Export-maximizing leaf clusters with age-dependent assimilation (XA)

Figure 1A illustrates the relationship between leaf life span and total daily assimilation on the shoot, daily costs of leaf construction, and the difference between these which is the assimilate available for export. For a given set of parameter values (see figure legend), total assimilation declines as life span increases due to the presence of more old leaves; assimilation reaches half of maximum when $L/b = 1$ (i.e., $L = b$) and the last leaf exhibits zero carbon gain. Leaf construction costs decline as an inverse function of life span, because the costs of each leaf are amortized over a longer time period. Assimilate export is maximized at an intermediate leaf life span, with the optimal value (L*) found by differentiating Eq. 8a (Table 2) with respect to L, and solving for the maximum, providing the identical result as Kikuzawa (1991):

$$L^*_{XA} = \left(\frac{2bc}{a_0}\right)^{1/2} \tag{9}$$

However, this case predicts that optimal leaf number (N^*_{XA}) and birth rate (r^*_{XA}) are infinite, because there is no cost imposed by self-shading, so carbon gain increases indefinitely with increasing N (Eq. 8a). The predicted assimilation rate at the time of leaf death is:

$$a^*_{x,XA} = a_0 - \left(\frac{2a_0c}{b}\right)^{1/2} \tag{10}$$

For biologically reasonable parameter values, this value will generally be considerably greater than zero. For example, if $a_0 = 0.1$ g g^{-1} day^{-1}, $c = 3$ g g^{-1} and $b = 200$ days, then optimal leaf life span = 110 days and $a_x{}^*_{XA} = 0.045$ g g^{-1} day^{-1}, suggesting that the leaf would be dropped while maintaining 45% of its initial diurnal assimilation potential.

Extension-maximizing shoots with position-dependent assimilation (RP)

Figure 1B illustrates the relationship of total leaf mass, mean assimilation rates and the resulting total daily assimilation, as a function of leaf number. Leaf production rate is proportional to total assimilation, so optimal leaf number is found at the maximum assimilation value. As leaf number increases, leaf mass increases but mean assimilation rates decline due to self-shading. The product of these two is maximal when mean assimilation rates drop to half of their initial value, and as found by solving Eq. 8d this corresponds to a simple prediction for optimal leaf number to maximize leaf production rates:

$$N^*_{RP} = p \tag{11}$$

This result indicates that $a_x{}^*_{RP}$ equals 0, so leaves are expected to be maintained only as long as they have a positive carbon balance. For a given number of leaves, leaf birth rate is maximized by maximizing allocation to new leaf production, and consequently minimizing leaf life span. From Eqs. 1, 5, and 7b:

$$L^*_{RP} = \frac{2c}{F_{\max}a_0} \tag{12}$$

where $F_{\max}$ is the maximum possible leaf allocation, constrained by stem, root, and other growth require-

Fig. 1 Graphical presentation of optimal solutions (*arrows*) for the XA and RP models. **A** XA model. Total assimilation (D_g), cost of new leaf construction (D_c), and assimilate export from shoot (D_s) as a function of leaf life span relative to the age at which assimilation reaches zero (L/b). The optimal solution maximizes D_s. Parameter values used for calculations (see Table 1 for definitions): $N = 10$, $a_0 = 0.15$ g g^{-1} day^{-1}, $c = 2.5$ g g^{-1}, $m = 1$ g. **B** RP model. Total leaf mass (N^*m), mean assimilation rate (a_m), and total shoot assimilation (D_g) as a function of leaf number relative to leaf position at which assimilation reaches zero (N/p). The optimal solution maximizes leaf production rate, which is proportional to D_g. Parameter values for calculations: $a_0 = 0.15$ g g^{-1} day^{-1}, $m = 1$ g

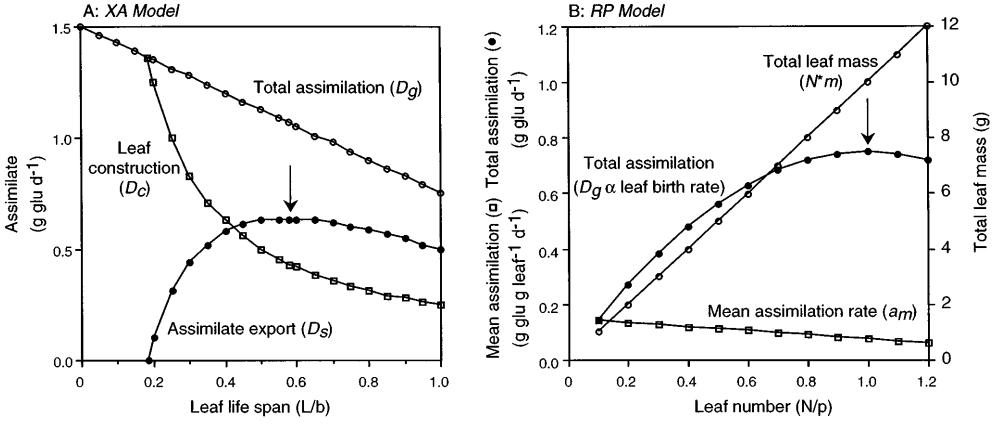

ments. Leaf birth rate on an extension-type shoot with optimal leaf number and life span is:

$$r^*_{RP} = \frac{N^* F_{\max} a_0}{2c} \quad (13)$$

and is therefore directly proportional to increases in assimilation, leaf number or proportional allocation to new leaves. Thus, the RP model provides finite predictions for all aspects of leaf cluster dynamics. In addition, the prediction of the RP model that a_x should equal 0 is both directly testable and intuitively appealing because it implies that leaves are not discarded while they maintain positive carbon balance, in contrast to the XA model above. (Note that the optimality functions are fairly flat around the optimum in both models, so the predicted reduction in performance due to moderate deviations from optimum behavior will be small).

Carbon gain and leaf dynamics of tropical pioneer trees: a test of the model

Optimality models may be tested using patterns of variation both within and among species. Intraspecific tests, particularly if the individuals are isogenic, explicitly examine environmentally induced variation and ask whether the plasticity in physiology and development conforms to predicted optimal behavior. In contrast, interpopulational or interspecific tests examine genetically based variation (if individuals are studied in similar environments), under the supposition that natural selection has shaped the differences among species in accord with predictions of the model. Interspecific comparisons introduce an additional variable, as different species may have evolved under divergent selection regimes, so predictions of a particular model may be confirmed in some species but not others. However, if optimal or near optimal behavior is observed across a range of species, the results provide greater confidence in the generality of the model. The optimality model presented here is explicitly formulated for a particular functional group of plants (plants with continuous leaf birth and death), so I have chosen to test the predictions based on patterns of interspecific variation among several species of tropical pioneer trees that exhibit such behavior. The goals of this field study were: (1) to obtain quantitative values for all directly measurable variables in the model, and from these to estimate values for the other major parameters, and (2) to test directly the predictions of optimal leaf number and life span and assimilation at leaf death, in order to determine which model is most consistent with observed behavior, and which may be rejected, for these species.

Materials and methods

Carbon assimilation and leaf dynamics were measured on small saplings of three species of pioneer trees, *Carica papaya* L. (Caricaceae), *Cecropia obtusifolia* Bertol. (Moraceae), and *Hampea nutricia* Fryx (Malvaceae) (henceforth referred to by their generic names), at the Los Tuxtlas Tropical Biology Station, Veracruz, Mexico (see Bongers et al. 1988 for site description). These three species germinate in or around the edges of recent tree fall gaps, grow rapidly in height, begin flowering after several years and complete their life cycles within 5 (*Carica*) to 30 (*Cecropia*) years (Sarukhán et al. 1985). *Carica* and *Cecropia* seedlings and saplings provide ideal study systems due to the absence of branching, while *Hampea* does not branch until it reaches 1–2 m in height. With regard to this study, the most interesting difference among the species is the variation in standing leaf numbers, ranging from approximately 5 in *Cecropia* to as high as 30 in *Hampea*. The study was conducted on a total of 13 individuals of the three species (4 *Carica*, 6 *Cecropia*, and 3 *Hampea*), located in three forest gaps in which several saplings were growing in close proximity, thus facilitating gas exchange measurements. The three species were chosen for study in order to obtain a greater range of parameter values and a broader test of the model predictions. Logistic constraints limited the scope of this field study, and the results should be considered a preliminary test of the model.

Leaf carbon balance

Diurnal carbon balance was measured on four to six (usually five) leaves on each plant. On each plant, the leaves chosen for measurement were distributed along the shoot from top to bottom, starting with an expanding or just expanded leaf and including the last standing leaf on the shoot. Measurements were made with a Li-Cor 6200 Photosynthesis System (Li-Cor, Lincoln, Neb.) operating in differential mode. Diurnal curves of net instantaneous photosynthetic rates were obtained on 22 March (site A), 24 March (site B), and 26 March (site C) 1993, with four, six, and five measurements on each leaf, respectively, across the day. Dark respiration rates were measured at dawn and/or dusk, after initial measurements indicated that rates varied little during the night (see Fig. 2). Measurements of very low gas exchange rates with the Li-Cor 6200 are very sensitive to small leaks in the system, but the cumulative impact of such errors is minimal on the overall analysis in this study. Photosynthetic measurements were made at ambient photosynthetic flux density (PFD) levels, with leaves maintained in their natural orientation. There were no significant differences in CO_2, temperature, and relative humidity recorded during the measurements at each site. Values of PFD at measurement were

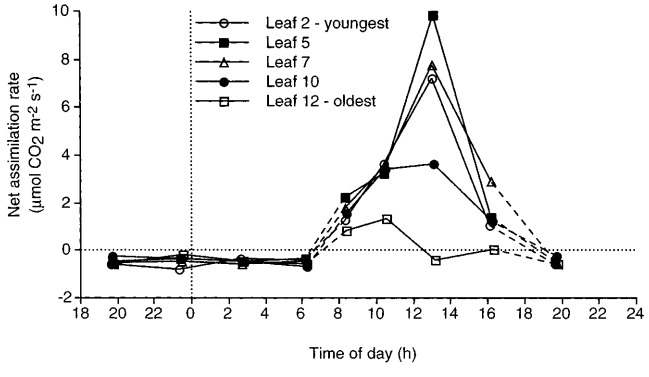

Fig. 2 Diurnal course of net carbon assimilation rates, illustrated for five leaves of one *Carica* papaya sapling. Night respiration measurements were collected overnight on 20–21 March 1993 and daytime photosynthetic measurements were made on 22 March 1993. The final respiration point at 2000 hours on the second day is duplicated from the initial measurement at the same time to complete the 24-h cycle. *Dotted lines* indicate connections between non-contiguous measurements. Diurnal net carbon gain (Fig. 3) was estimated as the area under these curves, relative to zero, times leaf mass per area of each leaf

highly variable due to differences among days in weather, among sites in the geometry of the canopy openings above the plants, and among leaves due to patterns of self-shading. Site C was measured on a predominantly overcast day, and overall PFD levels and assimilation rates were lower. Total diurnal assimilation (A/area) was determined as the area under the diurnal course of photosynthetic rates measured on each leaf. Leaf disks were removed from the lamina of each leaf in order to determine leaf mass per area (LMA), which was used to convert A/area to A/mass [g glucose (g leaf biomass)$^{-1}$ day^{-1}].

Initial assimilation rates (a_0) were calculated for each plant based on the highest value of A/mass, which was generally observed on the second leaf from the top, of those chosen for measurement, though occasionally it was the first or third leaf. Starting from this leaf, a linear regression of A/mass in relation to leaf position was used to estimate p, the position at which assimilation reaches zero. The leaf age at which assimilation reaches zero (b) was calculated as p times the mean age interval between successive leaves on each plant (= the inverse of the leaf birth rate). The regression was also used to estimate daily assimilation rate at abscission (a_x), by calculating assimilation at $N_x + 0.5$, where N_x is the position of the last leaf on the plant. Predicted values of L^*, N^* and a_x^* were calculated from values of p, b, a_0, and c obtained for each plant, based on the solutions of the model (Eqs. 9, 10, and 11).

Leaf dynamics and biomass allocation

A permanent ink mark was placed at the node of the lowest leaf in the cluster, and the total number of nodes (P_1) and standing leaves (N_1) was counted. After 30 days, the total number of leaves and nodes above the same mark was counted again for calculations of leaf dynamics parameters. Leaf birth rate over this interval was calculated from the increase in node numbers [$r = (P_2 - P_1)/t$], and leaf death rate from birth rate and the change in standing leaf numbers [$d = r - (N_2 - N_1)/t$]. Leaf life span was calculated following Eq. 1, using $N = (N_1 + N_2)/2$. Construction and support cost per gram of leaf tissue (in g glucose g leaf^{-1}) were calculated from the mass of the leaf, petiole and internode, using the lowest leaf on the shoot to estimate cumulative investment in the support structures, with respiratory costs of 1.5 g glucose g tissue^{-1} for the leaf and 1.2 g g^{-1} for the petiole and internode (Williams et al. 1987; Griffin 1994).

Testing the models

Analysis of covariance was conducted to determine whether the relationship between predicted and observed values for leaf life span (XA model) and leaf number (RP model) was significant within species, and if so whether slopes differed among species. For direct tests of model predictions, the differences between observed and predicted values were compared using a nested analysis of variance, with individual plants nested within species, and the observed value versus the predicted value as a categorical factor (OP). (The nested design is employed in these analyses because the observed and predicted values are measured independently on each plant, so plant-to-plant variation needs to be taken into account to provide the most powerful test for differences between these values.) Initially, a full model was examined, including the species × OP and site × OP interaction terms to determine whether the magnitude of the difference between observed and predicted values differed among species or sites. If these interaction terms were not significant, they were removed to test the significance of the observed versus predicted differences. Note that the site term incorporates both spatial and temporal variation, as each site was measured on a different day.

Results

Leaf initiation rates and construction cost

The standing number of leaves per shoot, the rate of leaf production and leaf life span all varied significantly among the three species (Table 3). *Carica* had a greater leaf number and birth rate than *Cecropia*, resulting in similar leaf life span for these species. *Hampea* had twice as many leaves as *Carica*, and a slightly lower leaf birth rate, resulting in a considerably longer leaf life span than in the other two species. There was no significant difference between the number of leaf births and deaths on each plant over the 30-day measurement interval (nested analysis of variance, $F_{1,12} = 2.13$, $P > 0.1$), supporting the assumption of equilibrium leaf numbers. Cumulative investment in the petiole and internode during the lifetime of a leaf ranged from 0.31 to 1.55 g support structure per gram leaf in the ten individuals of *Carica* and *Cecropia*, compared to 2.4 g g^{-1} in *Hampea*, resulting in total construction costs (c) from 1.9 to 4.4 g glucose per gram leaf tissue.

Diurnal carbon assimilation

Maximum instantaneous net photosynthetic rates measured on each leaf during the course of the diurnal cycle

Table 3 Mean (SE) of leaf dynamics and carbon assimilation parameters in three species used in this study; symbols before names correspond to model parameters (see Table 1). A/mass refers to diurnal carbon assimilation per unit leaf mass. The F-value (with 2,8 degrees of freedom) refers to the species effect in a two-way analysis of variance with species (fixed effect) and site (random effect) as main factors, and no interaction (*n.s.* not significant; $^*P \le 0.05$; $^{**}P \le 0.01$; $^{***}P \le 0.001$)

Parameter	*Carica papaya* $N = 4$	*Cecropia obtusifolia* $N = 6$	*Hampea nutricia* $N = 3$	F-value
N: leaf number	13.6 (1.09)	6.6 (0.95)	27.2 (1.09)	393***
r: leaf birth rate (day^{-1})	0.185 (0.028)	0.086 (0.028)	0.118 (0.011)	18.7***
d: leaf death rate (day^{-1})	0.129 (0.013)	0.081 (0.014)	0.129 (0.032)	3.43 n.s.
L: leaf life span (days)	76.1 (7.18)	77.7 (7.67)	235 (28.3)	28.0***
c: leaf construction cost (g g^{-1})	2.72 (0.25)	2.17 (0.13)	4.39[a]	
a_0: A/mass of newly mature leaf (g glucose g^{-1} day^{-1})	0.216 (0.057)	0.100 (0.019)	0.102 (0.016)	4.44*
a_x: A/mass at leaf death (g glucose g^{-1} day^{-1})	0.0435 (0.024)	0.0044 (0.015)	0.0072 (0.0035)	1.84 n.s.
p: leaf position at A/mass = 0	14.7 (2.5)	7.1 (2.1)	32.1 (2.7)	244***

[a] Leaf construction cost could only be estimated independently for one individual of *Hampea*

varied from 0.25 to 13.7 μmol CO_2 m^{-2} s^{-1}, while night respiration rates varied from −0.06 to −1.9 μmol m^{-2} s^{-1} (e.g., Fig. 2). Respiration rates were highest on the youngest leaves, and maximum net photosynthetic rates were generally highest on the second measured leaf (from the apex). The integrated diurnal carbon balance ranged from −0.099 to 0.21 mol CO_2 m^{-2} day^{-1}, with the highest rates again observed at the second measured leaf. Leaf mass per area varied between 16.8 and 46.6 g m^{-2} across all leaves; LMA was higher in *Cecropia* and *Hampea* and there was no consistent pattern with leaf position (cf. Traw and Ackerly 1995). Diurnal carbon assimilation rates on a mass basis, the parameter used in the model, varied from −0.076 to 0.34 g glucose (g leaf biomass)$^{-1}$ day^{-1} (Fig. 3). With one exception, a negative daily carbon balance was observed only on the highest and lowest leaves selected for measurement on each shoot, and the maximum rates on each plant were observed in recently expanded leaves. The maximum rates observed on each shoot (from 0.025 to 0.34 g g^{-1} day^{-1}) were used as estimates of a_0 for each plant. Mean a_0 was higher in *Carica* than in the other two species (Table 3), and these differences were marginally significant. The decline in assimilation with leaf position was highly variable, but showed no consistent non-linear patterns (Fig. 3). Based on linear regressions, the leaf position at which assimilation would reach zero (p) ranged from 3.7 to 10 in *Cecropia*, from 12.4 to 18.2 in *Carica*, and from 30.3 to 35.2 in *Hampea* (Table 3), and the differences among species were highly significant. Estimated values of a_x, assimilation at leaf death (calculated by evaluating the regression equation at one-half position beyond the last leaf), averaged 0.015 g g^{-1} day^{-1}, with a range from −0.043 to 0.090 g g^{-1} day^{-1}, and there were no significant differences among species (Table 3). There were slight but significant differences in a_x among sites ($F_{2,12} = 6.7$, $P < 0.05$), with higher values recorded at site B.

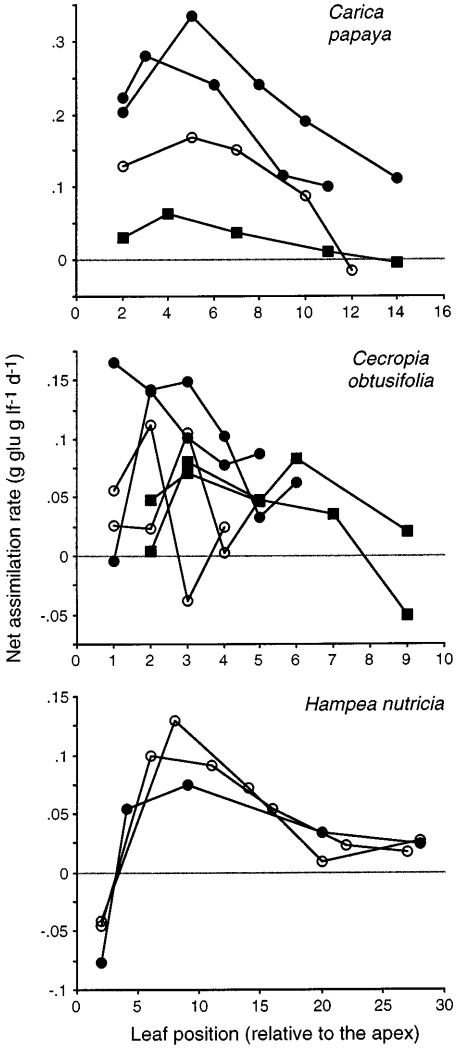

Fig. 3 Integrated net daily carbon gain for 13 individuals used in this study. Symbols indicate individuals measured in each of the three sites (*open circles* site A, *closed circles* site B, *squares* site C). From each curve, the highest observed value was used as an estimate of initial assimilation rates (a_0). A regression of assimilation on leaf position starting from the highest value was used to estimate the leaf position at which net assimilation would reach zero (p) and the assimilation rate at leaf abscission (a_x), as explained in the text

Comparison of results with model predictions

XA model

Predicted values of optimal leaf life span (L^*_{XA}) and assimilation at leaf death ($a_x{}^*_{XA}$) were calculated following Eqs. 9 and 10. Mean L^*_{XA} was significantly different among species ($F_{2,8} = 34.3$, $P < 0.001$), but effects of site were not significant. Predicted values of leaf life span (L^*_{XA}) showed no relationship with observed values (L) within species (ANCOVA, results not shown). The critical test of the model rests on the quantitative difference between observed and predicted values, and the significance of these differences. Observed L was 24, 50, and 60% greater than predicted L^*_{XA} in *Carica*, *Cecropia*, and *Hampea*, respectively (Fig. 4A), and the overall differences between observed and predicted values were significant (nested ANOVA,

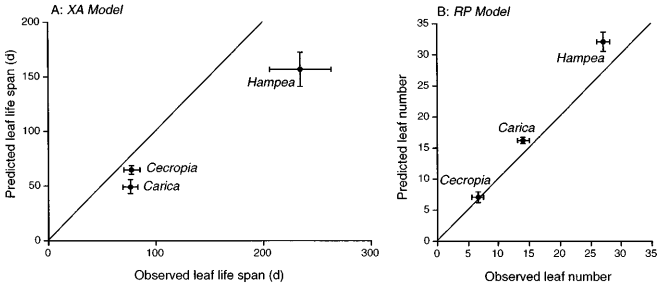

Fig. 4 Comparison of predicted and observed values for leaf life span under the XA model (**A**) and leaf number under the RP model (**B**). The *solid line* shows $x = y$, the expected relationship if observed values match model predictions

$F_{1,12} = 10.1$, $P < 0.01$). The magnitude of the differences between observed and predicted values did not differ significantly among species or sites (results not shown). Predicted values of assimilation at leaf death ($a_x{}^*_{XA}$) also exhibited no association with observed values (a_x) within species (ANCOVA, results not shown). Mean deviations of observed from predicted values ($a_x - a_x{}^*_{XA}$) averaged −0.059, -0.027, and −0.037 g g^{-1} day^{-1} for *Carica*, *Cecropia*, and *Hampea*, respectively (Fig. 5). Observed and predicted values were significantly different ($F_{1,12} = 16.7$, $P = 0.0015$), and the magnitude of the differences did not vary among species or sites (results not shown). The estimated reduction in assimilate export due to non-optimal leaf life span, calculated from Eq. 8a, was 12, 18, and 11% for *Carica*, *Cecropia*, and *Hampea*, respectively.

RP model

Optimal leaf number (N^*_{RP}) under the RP model is equivalent to p, the leaf position at which assimilation reaches zero. Variation in N^*_{RP} within species was not significantly associated with observed leaf numbers (ANCOVA, results not shown). Overall, observed values were slightly less than predicted values (average differences of 5.2, 4.6, and 15% in *Carica*, *Cecropia*, and *Hampea*, respectively; Fig. 4B). In the nested ANOVA, the species × OP and site × OP interactions were both significant ($F_{2,8} = 6.4$, $P < 0.05$; $F_{2,8} = 8.2$, $P < 0.05$, respectively). The species × OP interaction reflects the increasing divergence between observed and predicted values from *Cecropia* to *Carica* and *Hampea* (Fig. 4B). Observed values were 15% greater than predicted values in site C, and 5 and 23% less than predicted values in sites A and B, respectively, leading to the significant site × OP interaction. Most importantly, the difference between observed and predicted values for leaf number was not significant in the full model including interactions [$F_{1,2} = 1.7$, $P < 0.5$ (the low denominator *df* in the *F*-value corresponds to the site × OP term in the linear model)], though it was almost significant when interaction terms were removed ($F_{1,12} = 4.4$, $P = 0.058$). The reduction in leaf birth rates due to the small deviation of leaf numbers from the optimal prediction (from Eq. 8d) was 4, 5, and 3% in *Carica*, *Cecropia*, and *Hampea*, respectively. These values are lower than the predicted reductions in export, despite the relatively flat optimality curves in both models (Fig. 1A).

The predicted value of $a_x{}^*_{RP}$ was 0. Observed values of a_x ranged from −0.043 to 0.090 g g^{-1} day^{-1}, with higher mean values for *Carica* (Fig. 5). In the nested ANOVA, there was a significant site × OP interaction ($F_{2,8} = 6.7$, $P < 0.02$), as mean a_x was greater than 0 in site C (measured on an overcast day) and less than 0 in sites A and B. The differences between observed and predicted values were not significant when tested with or without interaction terms in the ANOVA model ($F_{1,2} = 0.51$, $p > 0.5$; $F_{1,12} = 2.5$, $P > 0.1$, respectively).

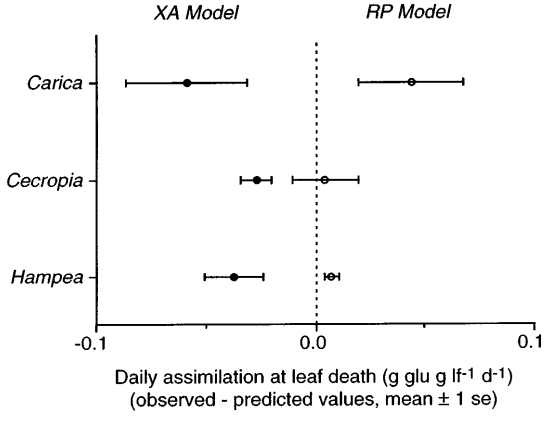

Fig. 5 Mean differences (±1 SE) between observed and predicted values of daily assimilation rate at the time of leaf death (a_x), under the XA and RP models. The *dotted line* at zero shows the expectation if observed values match model predictions. For the RP model, the predicted value = 0, so the results shown here are the measured values of a_x (Table 3)

Discussion

The primary goal of this study was to construct a quantitative model of leaf dynamics and carbon gain for tropical trees with continuous leaf production, and to examine the consequences of altering two aspects of the model: the mechanisms of declining carbon assimilation rates and the optimality criterion which is assumed to be maximized by the shoot. Three independent lines of reasoning provide strong support for the RP model, in which assimilation rates decline as a function of leaf position rather than age, and leaf dynamics maximize the rate of leaf production at the shoot apex, rather than net carbon export by the shoot. (1) As outlined in the Introduction, the effect of leaf position on assimilation (via self-shading) and the importance of height growth in the life history of pioneer trees are both strongly supported by various lines of physiological and ecological research. Thus the premises of the RP model are well supported on prior grounds. (2) Of the four model scenarios considered here, only the RP model provides finite, and therefore realistic, predictions for all aspects of leaf cluster structure and dynamics; the alternative models predict that either leaf life span or leaf number should be infinite, suggesting at the very least that these models are incomplete. (3) Finally, the preliminary test of the models presented here, using saplings of three tropical pioneer tree species, provides empirical support for the predictions of the RP model, as outlined above. This study was conducted on a relatively small number of plants and involved measurement of several variables each of which introduces some variability, potentially reducing the power of the statistical analyses to discriminate among the models. Despite this low power, the data were sufficient to reject the XA model, based on

significant differences between observed and predicted values. The data were more closely consistent with predictions of the RP model, though this consistency does not by itself confirm the model.

The empirical test of this model involves the measurement or estimation of a large number of physiological parameters, and as in all studies of leaf costs and benefits, there are many simplifying assumptions and sources of uncertainty in the actual measurements. The predictions of the XA model involve several parameters, including a_0 (initial assimilation rate of a newly expanded leaf), c (leaf construction cost), and b (the age at which assimilation is expected to reach zero). The variation between species was qualitatively consistent with the resulting predictions (Fig. 4A), but there was a significant quantitative discrepancy. Kikuzawa and Ackerly (in press) tested this model using published data for a broad range of species (including several with seasonal growth patterns which do not fit the approach taken here) and found a good fit to the predicted slope of 1/2 on a log-log scale, but the predicted optimal life span values were consistently lower than observed values, as in this study. In contrast, the critical prediction of the RP model is that leaves will be dropped when they reach zero carbon balance (or equivalently when $N = p$), so the calculation of assimilation rates and construction costs do not influence the results. This prediction is also consistent with the intuitive idea that leaves should not be dropped while they still exhibit a positive daily carbon balance, and the observations obtained in this study fit this prediction much more closely than those of the previous XA model.

In this study, carbon gain was estimated from nondestructive in situ measurements, allowing continued monitoring of leaf dynamics on the same plants. Ideally, assimilation would be measured on each plant on a representative range of days with varying weather conditions. This was not possible in this study, and in site C, the third day of assimilation measurements was overcast, leading to reduced assimilation rates (see Fig. 3). Reduced light levels are expected to cause greater proportional reductions in photosynthesis than respiration, and this would lead to a reduced x-intercept in the plot of diurnal assimilation versus leaf position. This pattern would be consistent with the result that observed leaf numbers were greater than predicted values (under the RP model) in site C, but less than predicted values in the other two sites (and vice versa for estimates of assimilation at leaf death). It is impossible, from these data, to determine whether the remaining discrepancies between observed and predicted values are due to additional factors that have not been included in the model, or to imprecise measurement of the relevant parameters. This question would be best addressed in the field with greater replication and data collection over a longer time period, or in the greenhouse with more precise control of environmental conditions and manipulation of the environment to alter predicted plant behavior (e.g., Ackerly and Bazzaz 1995a). In addition, it would be valuable to conduct detailed studies of a single species growing under a range of conditions to determine whether this model can account for intraspecific variation in leaf dynamics.

The assumption of a linear decline in assimilation rates was made both for algebraic simplicity and as an approximation of observed patterns. If assimilation initially declined less rapidly, and then dropped off rapidly as leaves senesced (cf. Kitajima et al. 1997), optimal leaf life span under the XA model and leaf number under the RP model would be increased, which would bring observed and predicted values more in line for the former (see Fig. 4). However, mean assimilation rates would have to be increased by 1.5- to 2.5-fold to make predicted leaf life span in the XA model as high as the observed values, and this is a greater discrepancy than that introduced by the assumption of linearity. If the decline in assimilation was more exponential, as the decline in light should be in a closed stand, then predicted leaf life spans under the XA model would be even shorter, increasing the discrepancy between predicted and observed values. The observed patterns included both slow and rapid initial decline (e.g., *Carica* and *Cecropia* vs *Hampea*), as well as non-monotonic patterns in several *Cecropia* (Fig. 3), so the linear pattern provided the simplest approximation to encompass this variability.

The construction costs associated with the production of a new leaf can be calculated in different ways (though as noted this does not influence the RP model). In particular, leaf production requires growth of new roots to maintain an active supply of water and soil nutrients, and height growth also requires continued investment in support structures in the trunk and subtending branches below a leaf cluster. In this model, these costs are included in the carbon exported from the leaf cluster (D_s), rather than treated as costs associated directly with leaf production. The costs of support and conducting structures are expected to increase with plant height (Givnish 1982, 1988). Increasing support costs in larger plants lead to a prediction of greater leaf life span in adults compared to seedlings (under either model considered here), as observed for a number of temperate tree species (Kikuzawa and Ackerly, in press). If these costs are included in the construction cost per leaf, then the net 'profits' of leaf assimilate would be those invested in new branch initiation and reproduction. Such an approach may prove useful to extend the approach here to include more complex canopies and the reproductive component of the life cycle, though it becomes increasingly difficult to obtain empirical measures corresponding to costs and benefits defined in this way.

The conceptual scheme of the RP model (illustrated in Fig. 6) is as follows. (1) The interaction of canopy structure and the local light environment determines the pattern of shading and distribution of assimilation rates among leaves on the shoot, such that the decline in assimilation is dependent on leaf position rather than age. (2) Leaves are maintained until the daily carbon balance

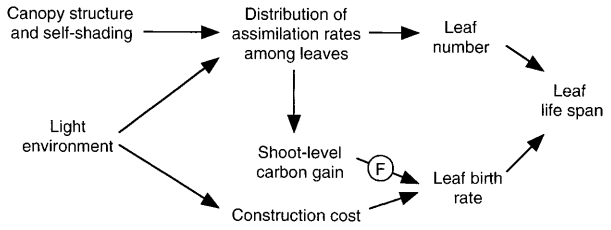

Fig. 6 Conceptual scheme of leaf dynamics in an extension-maximizing shoot with position-dependent assimilation (RP model), as supported by results of this study (see Discussion)

reaches zero, and this determines the number of leaves maintained on the shoot. (3) Shoot-level carbon gain is the sum of the assimilation rates of individual leaves, and a proportion (F) of this carbon is allocated to new leaf production, while the remainder is invested in stem and root growth, initiation of new leaf clusters (i.e., branching), and reproduction in mature plants. (4) Leaf birth rate is determined by the ratio of carbon assimilated to leaf production and the mean construction cost per leaf (leaf size influences both total assimilation and total cost per leaf so it cancels out of the final equations; see above). (5) Leaf life span then emerges as the ratio of leaf number to birth rate, following Eq. 1. The model does not focus on optimal leaf life span per se. Rather, the short leaf life span observed in tropical pioneer trees results from constraints on leaf number due to self-shading together with selection for rapid leaf production and extension growth. However, it is worth noting that leaf number does not ultimately enter into the predicted, optimal leaf life span. Rather, the role of assimilation rate and leaf construction cost result in strong associations of leaf life span with plant life history, environment, and growth rate (Reich et al. 1992, 1997). In contrast, the number of leaves per leaf cluster varies within life history groups, but does not show consistent patterns between groups (Ackerly 1996). Based on the model presented here (Fig. 6), leaf number reflects self-shading patterns within the shoot; these in turn are determined by various facets of canopy geometry, including leaf size, shape and orientation, petiole length and orientation, phyllotaxy, internode length and shoot orientation, together with the spatial structure of the light environment (Niklas 1988; Takenaka 1994; Ackerly and Bazzaz 1995b; Pearcy and Yang 1996). For example, among the tropical pioneers of the Los Tuxtlas forest, leaf numbers are lowest (3–4) in *Piper auritum*, with large leaves, short petioles and 1/3 phyllotaxy (Ackerly and Bazzaz 1995b), and highest (25–30) in *Hampea nutricia*, with 3/8 phyllotaxy, intermediate leaf size, and elongated petioles on lower leaves (Table 3 and personal observations). The adaptive significance (or lack thereof) of such variation in species with relatively similar life histories, remains largely unexplored (cf. Ackerly 1996).

The empirical support for the RP model in this study may reflect particular aspects of the biology of pioneer trees. First, leaf position changes rapidly in fast-growing plants, so the influence of positional processes may be stronger than any underlying age-related processes of physiological deterioration or chronological senescence. The relationship between leaf position and light levels is also more marked in vertically oriented (orthotropic) branches, which promotes a successive leafing strategy in vigorously growing early successional plants (Kikuzawa et al. 1996). In contrast, age-related senescence processes may be more important in slower-growing species with longer-lived leaves, species with determinate leaf flushes, and species with more horizontally oriented (plagiotropic) branches (cf. Kitajima et al. 1997). Secondly, the model presented here shifts the focus from individual leaf behavior to the dynamics of the entire leaf cluster at the tip of each shoot. In this context, carbon gain is interpreted as export of carbon from the base of the cluster to the remainder of the plant, after allocating assimilate for in situ leaf production. Thus, while the leaf may be considered primarily as a carbon-gaining organ, the leaf cluster as a whole acts as a unit of growth and extension of the canopy, making it possible to define the alternative optimality criteria considered here. For pioneer trees, height growth strongly influences survival and eventual reproductive success (Augspurger 1984; Brokaw 1987) and is almost certainly more important than carbon export from the terminal leaf cluster. However, for slower-growing species and for the determinate short shoots exhibited by some tree species, the export-maximizing criterion may be more appropriate. Further development of the general model, relaxing the assumptions of equilibrium leaf numbers and an aseasonal environment, may lead to additional testable predictions that can be applied to other species.

Acknowledgments I am indebted to Doug Karpa, Paul Voss, and Horacio Paz for their assistance in the field, and to the staff of the Los Tuxtlas Biological Station for providing facilities for field work. This work has benefited greatly from discussions with Kihachiro Kikuzawa; comments from Niels Anten, Susan Bassow, Fakhri Bazzaz, Stuart Davies, Miguel Martínez-Ramos, and anonymous reviewers greatly improved the manuscript. This research was funded by a National Science Foundation Doctoral Dissertation Improvement Grant.

References

Ackerly DD (1993) Phenotypic plasticity and the scale of environmental heterogeneity: studies of tropical pioneer trees in variable light environments. PhD thesis, Harvard University, Cambridge, Mass

Ackerly DD (1996) Canopy structure and dynamics: integration of growth processes in tropical pioneer trees. In: Mulkey SS, Chazdon RL, Smith AP (eds) Tropical forest plant ecophysiology. Chapman & Hall, London, pp 619–658

Ackerly DD, Bazzaz FA (1995a) Leaf dynamics, self-shading and carbon gain in seedlings of a tropical pioneer tree. Oecologia 101:289–298

Ackerly DD, Bazzaz FA (1995b) Seedling crown orientation and interception of diffuse radiation in tropical forest gaps. Ecology 76:1134–1146

Alvarez-Buylla ER, Martínez-Ramos M (1992) Demography and allometry of *Cecropia obtusifolia*, a neotropical pioneer tree – an evaluation of the climax-pioneer paradigm for tropical rain forests. J Ecol 80:275–290

Augspurger CK (1984) Light requirements of neotropical tree seedlings: a comparative study of growth and survival. J Ecol 72:777–795

Bongers F, Popma J, Meave del Castillo J, Carabias J (1988) Structure and floristic composition of the lowland rain forest of Los Tuxtlas, Mexico. Vegetatio 74:55–80

Brokaw NVL (1987) Gap-phase regeneration of three pioneer species in a tropical forest. J Ecol 75:9–19

Chabot BF, Hicks DJ (1982) The ecology of leaf life spans. Annu Rev Ecol Syst 13:229–259

Field CB (1983) Allocating leaf nitrogen for the maximization of carbon gain: leaf age as a control on the allocation program. Oecologia 56:341–347

Fisher JB (1986) Branching patterns and angles in trees. In: Givnish TJ (ed) On the economy of plant form and function. Cambridge University Press, Cambridge, UK, pp 493–524

Givnish TJ (1982) On the adaptive significance of leaf height in forest herbs. Am Nat 120:353–381

Givnish TJ (1988) Adaptation to sun and shade: a whole plant perspective. Aust J Plant Physiol 15:63–92

Griffin KL (1994) Calorimetric estimates of construction cost and their use in ecological studies. Funct Ecol 8:551–562

Hensel LL, Grbic V, Baumgarten DA, Bleecker AB (1993) Developmental and age-related processes that influence the longevity and senescence of photosynthetic tissues in *Arabidopsis*. Plant Cell 5:553–564

Hikosaka K, Terashima I, Katoh S (1994) Effects of leaf age, nitrogen nutrition and photon flux density on the distribution of nitrogen among leaves of a vine (*Ipomoea tricolor* Cav.) grown horizontally to avoid mutual shading of leaves. Oecologia 87:451–457

Hirose T, Werger MJA, Pons TL, Rheenen JWA van (1988) Canopy structure and leaf nitrogen distribution in a stand of *Lysimachia vulgaris* L. as influenced by stand density. Oecologia 77:145–150

Kikuzawa K (1991) A cost-benefit analysis of leaf habit and leaf longevity of trees and their geographical pattern. Am Nat 138:1250–1263

Kikuzawa K (1995) The basis for variation in leaf longevity in plants. Vegetatio 122:89–100

Kikuzawa K, Ackerly DD (in press) Significance of leaf longevity in plants. Pl Sp Biol

Kikuzawa K, Kudo G (1995) Effects of the length of the snow-free period on leaf longevity in alpine shrubs: a cost-benefit model. Oikos 73:214–220

Kikuzawa K, Koyama H, Umeki K, Lechowicz MJ (1996) Some evidence for an adaptive linkage between leaf phenology and shoot architecture in sapling trees. Funct Ecol 10:252–257

Kitajima K, Mulkey SS, Wright SJ (1997) Decline of photosynthetic capacity with leaf age in relation to leaf longevities for five tropical canopy tree species. Am J Bot 84:702–708

Mooney HA, Field C, Gulmon SL, Bazzaz FA (1981) Photosynthetic capacity in relation to leaf position in desert versus old-field annuals. Oecologia 50:109–112

Niklas K (1988) The role of phyllotactic pattern as a "developmental constraint" on the interception of light by leaf surfaces. Evolution 42:1–16

Pearcy RW, Yang W (1996) A three-dimensional crown architecture model for assessment of light capture and carbon gain by understory plants. Oecologia 108:1–12

Reich PB, Walters MB, Ellsworth DS (1992) Leaf life-span in relation to leaf, plant, and stand characteristics among diverse ecosystems. Ecol Monogr 62:365–392

Reich PB, Walters MB, Ellsworth DS (1997) From tropics to tundra: global convergence in plant functioning. Proc Natl Acad Sci USA 94:13730–13734

Sarukhán J, Piñero D, Martínez-Ramos M (1985) Plant demography: a community-level interpretation. In: White J (ed) Studies on plant demography: a festschrift for John L. Harper. Academic Press, London, pp 17–31

Sobrado MA (1991) Cost-benefit relationships in deciduous and evergreen leaves of tropical dry forest species. Funct Ecol 5:608–616

Takenaka A (1994) Effects of leaf blade narrowness and petiole length on the light capture efficiency of a shoot. Ecol Res 9:109–114

Traw MB, Ackerly DD (1995) Leaf age, light levels and nitrogen allocation in five species of rain forest pioneer trees. Am J Bot 82:1137–1143

Williams K, Percival F, Merino J, Mooney H (1987) Estimation of tissue construction cost from heat of combustion and organic nitrogen content. Plant Cell Environ 10:725–734

Williams K, Field CB, Mooney HA (1989) Relationships among leaf construction cost, leaf longevity, and light environments in rain-forest plants of the genus *Piper*. Am Nat 133:198–211

Witkowski ETF, Lamont BB, Walton CS, Radford S (1992) Leaf demography, sclerophylly and ecophysiology of two *Banksias* with contrasting leaf life spans. Aust J Bot 40:849–862